



HAL
open science

Hybrid light-matter states in topological superconductors coupled to cavity photons

Olesia Dmytruk, Marco Schirò

► **To cite this version:**

Olesia Dmytruk, Marco Schirò. Hybrid light-matter states in topological superconductors coupled to cavity photons. 2023. hal-04480983

HAL Id: hal-04480983

<https://hal.science/hal-04480983>

Preprint submitted on 27 Feb 2024

HAL is a multi-disciplinary open access archive for the deposit and dissemination of scientific research documents, whether they are published or not. The documents may come from teaching and research institutions in France or abroad, or from public or private research centers.

L'archive ouverte pluridisciplinaire **HAL**, est destinée au dépôt et à la diffusion de documents scientifiques de niveau recherche, publiés ou non, émanant des établissements d'enseignement et de recherche français ou étrangers, des laboratoires publics ou privés.



Distributed under a Creative Commons Attribution 4.0 International License

Hybrid light-matter states in topological superconductors coupled to cavity photons

Olesia Dmytruk^{1,2} and Marco Schirò²

¹ CPHT, CNRS, École Polytechnique, Institut Polytechnique de Paris, 91120 Palaiseau, France

² JEIP, UAR 3573 CNRS, Collège de France, PSL Research University,
11 Place Marcelin Berthelot, 75321 Paris Cedex 05, France

(Dated: October 11, 2023)

We consider a one-dimensional topological superconductor hosting Majorana bound states at its ends coupled to a single mode cavity. In the strong light-matter coupling regime, electronic and photonic degrees of freedom hybridize resulting in the formation of polaritons. We find the polariton spectrum by calculating the cavity photon spectral function of the coupled electron-photon system. In the topological phase the lower in energy polariton modes are formed by the bulk-Majorana transitions coupled to cavity photons and are also sensitive to the Majorana parity. In the trivial phase the lower polariton modes emerge due to the coupling of the bulk-bulk transitions across the gap to photons. Our work demonstrates the formation of polaritons in topological superconductors coupled to photons that contain information on the features of the Majorana bound states.

I. INTRODUCTION

Cavity embedding provides a promising avenue to probe and control quantum materials and devices. On the one hand there is tantalizing possibility of controlling phase transitions and phase diagrams by coupling to a cavity mode, an idea which has received theoretical and experimental attention [1, 2]. Another source of cavity control can arise from the hybridization with finite-frequency modes, leading to new hybrid quasiparticles – polaritons [3], which can be then probed and control in novel ways. A wide range of polaritonic modes have been proposed and observed, classified depending on the type of charged particles in the matter component [4].

A particularly appealing scenario arises when the material has a non-trivial topological character, a feature which can then be enhanced or suppressed [5–9] or even generated by the coupling with a cavity and thus transmitted to the emergent polariton excitations [10]. Among topological phases of matter, topological superconductors hosting zero-energy Majorana bound states [11–14] hold a specially interesting place for their potential for quantum computing [15]. The prototype system for topological superconductivity is the Kitaev chain model [11] describing a one-dimensional p -wave superconductor with Majorana bound states emerging at its opposite ends in the topological phase. Promising platforms for the Majorana bound states are superconductor-semiconductor nanowires [16, 17], graphene-like systems [18, 19], and chains of magnetic atoms [20–22]. Signatures of the Majorana bound states in the form of zero-bias peak have been experimentally observed in superconductor-semiconductor nanowire platforms [23–29]. However, theoretical works have demonstrated that the zero-bias peak could arise due to non-Majorana mechanisms [30–38].

The idea of using cavities to probe and manipulate the Majorana bound states has been explored in different settings [39–47]. In these cases the cavity plays mainly the role of non-invasive spectroscopic tool to probe the physics of these modes. A different scenario arises poten-

tially in the strong or ultrastrong light-matter coupling regime where polariton modes are formed, which in the case of a topological superconductor could take the form of the Majorana polaritons [48, 49].

In this work we study the hybrid light-matter states that emerge by coupling topological superconductors to a single mode cavity. We consider two models of topological superconductors hosting the Majorana bound states: a prototype Kitaev chain model [11] and a more realistic nanowire model [16, 17]. Hybridization between electronic and photonic states results in formation of polaritons. We focus specifically on the signatures of these polaritonic modes which emerge in the cavity photon spectral function [7, 50–53], which is directly measurable in a transmission/reflection experiment [40, 54]. We find that the polariton spectrum is sensitive to the Majorana parity in the topological phase. Moreover, the energies of the polariton modes are different in the trivial and topological phases that could be used to probe the emergence of zero modes in topological superconductor.

The paper is organized as follows. In Sec. II we introduce two tight-binding models for topological superconductors and derive how to couple them to a single mode cavity. Then, in Sec. III we calculate the polariton spectrum of the coupled electron-photon system. Finally, Sec. IV is devoted to conclusions.

II. COUPLING TOPOLOGICAL SUPERCONDUCTORS TO LIGHT

We start by discussing how to couple topological superconductors described by a tight-binding model to a single mode cavity. We consider two models for topological superconductors: (1) a prototype Kitaev chain [11] and (2) an experimentally relevant nanowire with spin-orbit interaction and proximity-induced superconductivity subject to magnetic field [16, 17]. Contrary to previously studied tight-binding models for non-superconducting systems [7, 52], the Kitaev chain (nanowire) models contain p -wave (s -wave) superconducting pairing term that

pairs two neighboring sites (opposite spins) in the chain.

A. Kitaev chain coupled to cavity

The Hamiltonian for the Kitaev chain reads [11],

$$H_K = -\mu \sum_{j=1}^N c_j^\dagger c_j - t \sum_{j=1}^{N-1} (c_j^\dagger c_{j+1} + \text{h.c.}) + \Delta \sum_{j=1}^{N-1} (c_j c_{j+1} + \text{h.c.}), \quad (1)$$

where c_j^\dagger (c_j) are fermionic creation (annihilation) operators at site j , N is the total number of sites in the chain, μ is the chemical potential, t is the hopping amplitude, and Δ is a p -wave superconducting pairing potential. The Kitaev chain is in the topological (trivial) phase if $|\mu| < 2t$ ($|\mu| > 2t$) hosting two Majorana bound states describes by the operators $\gamma_{L(R)} = \gamma_{L(R)}^\dagger$. These two Majorana operators form a full fermionic state with $c_M = (\gamma_L - i\gamma_R)/2$ that gives raise to the Majorana occupation $n_M = \langle c_M^\dagger c_M \rangle$ that determines its parity. The Majorana occupation n_M can be 0 or 1 corresponding to the even (odd) parity.

Next, we couple the Kitaev chain to a single mode cavity given by the Hamiltonian $H_{ph} = \omega_c (a^\dagger a + 1/2)$, where a^\dagger (a) is the photonic creation (annihilation) operator and ω_c is the cavity frequency. The Kitaev chain Hamiltonian H_K is coupled to the electromagnetic field described by a homogeneous photonic vector potential $\mathbf{A} = \mathbf{u}_x (g/e) (a + a^\dagger)$ via the Peierls substitution, which is equivalent to applying a unitary transformation U to the electronic Hamiltonian (6) only [7, 52], $H_{K-ph} = H_{ph} + U^\dagger H_K U$, with

$$U = e^{i \frac{g}{\sqrt{N}} (a+a^\dagger) \sum_j R_j c_j^\dagger c_j}. \quad (2)$$

Here, $R_j = j - l_0$, where $l_0 = N/2$ for even N . Using that

$$U^\dagger c_m U = e^{i \frac{g}{\sqrt{N}} (a+a^\dagger) R_m} c_m, \quad (3)$$

we find that the superconducting pairing term acquires a site-dependent phase and the full light-matter Hamiltonian reads

$$H_{K-ph} = -\mu \sum_{j=1}^N c_j^\dagger c_j - \sum_{j=1}^{N-1} \left(t e^{i \frac{g}{\sqrt{N}} (a+a^\dagger)} c_j^\dagger c_{j+1} + \text{h.c.} \right) + \sum_{j=1}^{N-1} \left(\Delta e^{i \frac{g}{\sqrt{N}} (2R_j+1)(a+a^\dagger)} c_j c_{j+1} + \text{h.c.} \right) + \omega_c \left(a^\dagger a + \frac{1}{2} \right). \quad (4)$$

Moreover, we note that coupling the superconducting pairing term to light is equivalent to dressing Δ with a phase, $\Delta \rightarrow \Delta e^{i\varphi}$ [41, 55, 56]. The phase φ could be found under the assumption that the p -wave pairing term in H_K is inherited from the bulk s -wave superconductor underneath the wire. In this case, we consider that the instantaneous supercurrent flowing through the bulk superconductor vanishes,

$$J_s = \frac{2e}{m} |\psi|^2 (\nabla\varphi - 2e\mathbf{A}) \equiv 0. \quad (5)$$

Here, m , $|\psi|^2$, and φ are the electronic mass, the density of superconducting electrons in the s -wave superconductor, and its phase, respectively. The solution of the differential equation $\nabla\varphi = 2e\mathbf{A}$ gives us $\varphi_j = 2g(a + a^\dagger)(j - l_0 + 1/2)\sqrt{N}$. Here, φ_j is chosen such that $\varphi_1 = -\varphi_N$ [54]. We note that these two approaches result in the same light-matter Hamiltonian given by Eq. (4). Alternatively, light-matter coupling could be included in the problem by starting with a semiconducting nanowire tunnel coupled to a bulk s -wave superconductor and assuming that the tunneling hopping is dressed with the Peierls phase [40].

B. Superconductor-semiconductor nanowire coupled to cavity

We now consider a more realistic model of topological superconductor coupled to photonic cavity. The tight-binding Hamiltonian composed of N sites that describes a semiconducting nanowire with Rashba spin-orbit interaction and proximity-induced superconductivity subject to magnetic field reads [57]

$$H_{nw} = \sum_{j,\sigma,\sigma'} \left[c_{j+1,\sigma}^\dagger (-t\delta_{\sigma\sigma'} + i\alpha\sigma_{\sigma\sigma'}^y) c_{j,\sigma'} + \Delta c_{j,\uparrow}^\dagger c_{j,\downarrow}^\dagger + \frac{1}{2} c_{j,\sigma}^\dagger [(2t - \mu)\delta_{\sigma\sigma'} + V_Z\sigma_{\sigma\sigma'}^x] c_{j,\sigma'} + \text{h.c.} \right], \quad (6)$$

where $c_{j,\sigma}^\dagger$ ($c_{j,\sigma}$) is the creation (annihilation) operator acting on electrons with spin σ located at site j , $\sigma_{x(y)}$ is the x (y) Pauli matrix acting in the spin space, and $t = \hbar^2 / (2m^* a_l^2)$ is the hopping amplitude, with m^* the effective mass and a_l lattice constant. Here, α is the spin-orbit coupling, Δ is the proximity-induced superconducting pairing potential, μ is the chemical potential, and $V_Z = g^* \mu_B B / 2$ is the Zeeman energy, with g^* the g -factor of the nanowire and μ_B the Bohr magneton. The nanowire hosts Majorana bound states emerging at the opposite ends of the one-dimensional system if $V_Z > \sqrt{\Delta^2 + \mu^2}$ [16, 17].

Similarly to the Kitaev chain, the light-matter Hamiltonian for the nanowire coupled to a single mode cavity could be obtained by performing the unitary transformation $H_{nw-ph} = H_{ph} + U^\dagger H_{nw} U$, with

$$U = e^{i \frac{g}{\sqrt{N}} (a+a^\dagger) \sum_{j\sigma} \chi_j c_{j\sigma}^\dagger c_{j\sigma}}. \quad (7)$$

Here, $\chi_j = j - j_0$ is chosen such that $\chi_1 = -\chi_N$ [54], with $j_0 = (N + 1)/2$ for even N . Using that

$$U^\dagger c_{m\sigma'} U = e^{i\frac{g}{\sqrt{N}}(a+a^\dagger)\chi_m} c_{m\sigma'}, \quad (8)$$

we find that total light-matter coupling Hamiltonian becomes

$$\begin{aligned} H_{nw-ph} &= \sum_{j,\sigma,\sigma'} \left[c_{j+1,\sigma}^\dagger \left(-te^{-i\frac{g}{\sqrt{N}}(a+a^\dagger)} \delta_{\sigma\sigma'} \right. \right. \\ &+ i\alpha e^{-i\frac{g}{\sqrt{N}}(a+a^\dagger)} \sigma_{\sigma\sigma'}^y \left. \left. \right) c_{j,\sigma'} + \Delta e^{-2i\frac{g}{\sqrt{N}}\chi_j(a+a^\dagger)} c_{j,\uparrow}^\dagger c_{j,\downarrow}^\dagger \right. \\ &+ \left. \frac{1}{2} c_{j,\sigma}^\dagger [(2t - \mu) \delta_{\sigma\sigma'} + V_Z \sigma_{\sigma\sigma'}^x] c_{j,\sigma'} + \text{h.c.} \right] \\ &+ \omega_c \left(a^\dagger a + \frac{1}{2} \right). \end{aligned} \quad (9)$$

In the next section we will discuss the cavity photon spectral function for the two models in Eqs. (4) and (9) and highlight the emergence of polariton excitations and their topological signatures.

III. POLARITON SPECTRUM

In the strong light-matter coupling regime, the electronic and photonic states hybridize giving rise to the formation of new hybrid quasiparticles – polaritons. The polariton spectrum can be obtained by computing the cavity photon spectral function

$$A(\omega) = -\frac{1}{\pi} \text{Im} \int dt e^{-i\omega t} (-i\theta(t)) \langle [a(t), a^\dagger] \rangle. \quad (10)$$

To compute this quantity we follow Refs. [7, 50–52], write down the action for the electron-photon problem which we evaluate at the saddle point plus Gaussian fluctuations in the cavity field. Due to gauge-invariance the photon remains incoherent in presence of a uniform vector potential [52, 58–61]. The light-matter coupling however gives rise to a self-energy correction for the cavity mode arising from current-current fluctuations of the electronic system. As a result the cavity spectral function takes the form [7, 52]

$$A(\omega) = -\frac{1}{\pi} \frac{\chi''(\omega)(\omega + \omega_c)^2}{(\omega^2 - \omega_c^2 - 2\omega_c\chi'(\omega))^2 + (2\omega_c\chi''(\omega))^2}, \quad (11)$$

where $\chi(\omega) = K(\omega) - \langle J_d \rangle$ is the current-current correlation function, with

$$K(t - t') = -i\theta(t - t') \langle [J_p(t), J_p(t')] \rangle. \quad (12)$$

Here, J_p (J_d) are paramagnetic (diamagnetic) current operators that could be defined from the second-order expansion in g [7, 52]

$$H_{K(nw)-ph} \approx \omega_c a^\dagger a + H_{K(nw)} + (a + a^\dagger) J_p - \frac{(a + a^\dagger)^2}{2} J_d \quad (13)$$

and $\theta(t - t')$ is the Heaviside step function.

Polariton spectrum is approximately given by the solutions of the equation [52, 60]

$$\omega^2 \approx \omega_c^2 + 2\omega_c\chi'(\omega). \quad (14)$$

For $g = 0$ the topological superconductor and cavity photons are fully decoupled and there is a single solution of Eq. (14) given by $\omega = \omega_c$. For finite light-matter coupling $g \neq 0$ electrons and photons are coupled resulting in multiple solutions that depend both on cavity frequency ω_c and parameters of the electronic system through the real part of the current-current correlation function $\chi'(\omega)$. Therefore, the resulting polariton energies are sensitive to the properties of the topological superconductor.

We start by deriving the general expression for the current-current correlation function $\chi(\omega)$. Coupling between topological superconductor and cavity photons induces transitions between the Majorana and bulk states in the chain [40, 46, 47]. These Majorana-bulk transitions could be directly seen as peaks in the imaginary part of the correlation function $K(\omega)$ Eq. (12). To evaluate $K(\omega)$, we rewrite the fermionic operators c_j (c_j^\dagger) in terms of the annihilation (creation) operators \tilde{c}_n (\tilde{c}_n^\dagger) for the Bogoliubov quasiparticles [40, 46]

$$c_j = \sum_n (u_{j,n} \tilde{c}_n + v_{j,n} \tilde{c}_n^\dagger), \quad (15)$$

so that the electronic Hamiltonian (1) (6) becomes diagonal $\tilde{H}_{el} = \sum_n \epsilon_n (\tilde{c}_n^\dagger \tilde{c}_n - 1/2)$. Here, $u_{j,n}$ ($v_{j,n}$) are the electron (hole) components of the eigenvectors and ϵ_n are the corresponding eigenvalues of the electronic Hamiltonian, with $n = 1 \dots N$ for the Kitaev chain Hamiltonian (1) and $n = 1 \dots 2N$ for the superconductor-semiconductor nanowire Hamiltonian (6). To calculate the expectation value of the diamagnetic current operator $\langle J_d \rangle$ over a bare electronic Hamiltonian (1) (6) we rewrite J_d in terms of \tilde{c}_n (\tilde{c}_n^\dagger) operators and use that $\langle \tilde{c}_n^\dagger \tilde{c}_m \rangle = f(\epsilon_n) \delta_{n,m}$, with $f(\epsilon_m)$ being the Fermi distribution function. Assuming zero temperature, $f(\epsilon_m)$ reduces to the occupation number n_m that can take values 0 or 1 for empty or occupied state. Under this assumption, we arrive at the following expression

$$\langle J_d \rangle = \sum_m j_m^d n_m, \quad (16)$$

where j_m^d is the diagonal matrix element for the diamagnetic current operator between eigenstates corresponding to the eigenvalues ϵ_m . Defining the Fourier transformation as $K(\omega) = \int e^{i\omega t} K(t)$ and using that $\tilde{c}_m(t) = \tilde{c}_m(0) e^{-i\epsilon_m t}$, we find the general expression for the paramagnetic current correlation function at zero temperature

$$K(\omega) = \sum_{l,m} |j_{l,m}^p|^2 \frac{n_l - n_m}{\omega + \epsilon_l - \epsilon_m + i\eta}. \quad (17)$$

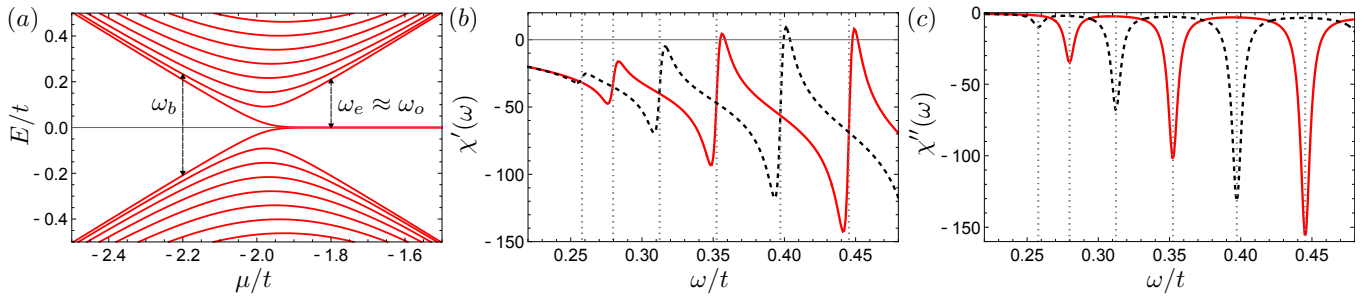


FIG. 1. (a) Energy spectrum of the Kitaev chain 1 as a function of the chemical potential μ/t (red solid lines). Vertical dashed lines indicate the transition frequencies ω_b and $\omega_{e(o)}$. For the chosen set of parameters Majorana energy $\epsilon_M = 7.44 \times 10^{-7}$ and $\omega_e \approx \omega_o$. (b) Real part of the current-current correlation function $\chi'(\omega)$ as function of frequency ω/t . Red solid (black dashed) lines correspond to even (odd) Majorana parity. The transition frequencies ω_e are shown in gray vertical dotted lines. (c) Imaginary part of the current-current correlation function $\chi''(\omega)$ as function of frequency ω/t for even (odd) Majorana parity shown in red solid (black dashed) lines. Gray vertical dotted lines correspond to the transition frequencies and indicate the position of the peaks. Parameters are chosen as $N = 100$, $\Delta/t = 1$, $\mu/t = -1.75$ (except in panel (a)), $\eta = 4 \times 10^{-3}$.

Here, $j_{l,m}^p$ are the matrix elements of the paramagnetic current and $\eta > 0$ is the linewidth of the energy levels. At zero temperature only bulk states with negative energies are occupied, while $n_l \equiv n_M = 0, 1$ for the Majorana states. We note that $K(\omega) = 0$ for $l = m$ making it fully off-diagonal in contrast to $\langle J_d \rangle$. When the system is in the topological phase the paramagnetic current correlation function given by Eq. (17) can be rewritten as a sum of three contributions $K(\omega) = K_{BB}(\omega) + K_{BM}(\omega) + K_{MM}(\omega)$, corresponding respectively to transitions between bulk states only (K_{BB}), between Majorana and bulk states (K_{BM}) and between Majorana states only (K_{MM}). We note that $K_{MM}(\omega) = 0$ since Majorana parity remains conserved in the presence of coupling to photons [40]. The bulk only contribution in the topological phase (or the total paramagnetic current correlation function in the trivial phase) could be further simplified to

$$K_{BB}(\omega) = \sum_{\epsilon_l \neq \epsilon_m > 0} \left(\frac{1}{\omega - \omega_b + i\eta} - \frac{1}{\omega + \omega_b + i\eta} \right) \times |j_{l,-m}^p|^2, \quad (18)$$

where $\omega_b = \epsilon_l + \epsilon_m$ is the transition frequency between the bulk states l and m , and $j_{l,-m}^p$ is the matrix element between the bulk states with energies ϵ_l and $-\epsilon_m$. The peaks in the imaginary part of the bulk contribution appear at transition frequencies $\omega_b > 2\Delta_g$, where Δ_g is the effective gap in the electronic energy spectrum.

Furthermore, the bulk-Majorana transitions are included in $K_{BM}(\omega)$ term given by

$$K_{BM}(\omega) = \sum_{\epsilon_l > 0} \left(\frac{1}{\omega - \omega_{e(o)} + i\eta} - \frac{1}{\omega + \omega_{e(o)} + i\eta} \right) \times \left[|j_{l,o}^p|^2 (n_M - n_l) + |j_{l,e}^p|^2 (1 - n_l - n_M) \right], \quad (19)$$

where $\omega_{e(o)} = \epsilon_l \pm \epsilon_M$ is the transition frequency between bulk state with occupation number $n_l = 0$ and Majorana

state with occupation number $n_M = 0(1)$ corresponding to even (odd) parity, and $j_{l,e(o)}^p$ is the matrix element between bulk state l and even e (odd o) parity Majorana state. The imaginary part of the paramagnetic current correlation function $K_{BM}''(\omega)$ calculated for even parity with $n_M = 0$ has multiple peaks at frequency $\omega_e > \Delta_g$ with the amplitude given by $|j_{l,e}^p|^2$, while for $n_M = 1$ the peaks are at ω_o with the amplitude given by $|j_{l,o}^p|^2$. Moreover, even in the absence of the overlap between two Majorana bound states $\epsilon_M \approx 0$ the correlation function $K_{BM}(\omega)$ distinguishes between different Majorana parities through the matrix elements $j_{l,e(o)}^p$ [46].

In the topological phase the cavity spectral function $A(\omega)$ given by Eq. (11) depends on the Majorana parity through the different matrix elements entering in the current-current correlation function $\chi(\omega)$ and, therefore, polariton spectrum could be used to probe Majorana properties. Comparing Eqs. (19) and (18) we note that the lowest-energy peaks in the topological and trivial phases appear at frequencies $\omega_{e(o)} \approx \Delta_g$ and $\omega_b \approx 2\Delta_g$, respectively, suggesting that the cavity spectral function could be also used to differentiate between two phases.

A. Polaritons in Kitaev chain coupled to photons

We start discussing the cavity spectral function for the Kitaev chain, Eq. (4). In this case the paramagnetic and diamagnetic current operators could be found from Eq. (4):

$$J_p = i \frac{g}{\sqrt{N}} \sum_j \left[-tc_j^\dagger c_{j+1} + 2\Delta(R_j + 1/2)c_j c_{j+1} - \text{h.c.} \right] \quad (20)$$

and

$$J_d = \frac{g^2}{N} \sum_j \left[-tc_j^\dagger c_{j+1} + 4\Delta(R_j + 1/2)^2 c_j c_{j+1} + \text{h.c.} \right], \quad (21)$$

where we see that in addition to the usual contribution from single particle hopping there is also a term coming from the superconducting pairing. We emphasize that this current is not associated to a conserved charged in the Kitaev model, which only enjoys a discrete Z_2 parity symmetry. However, it is the natural object entering the response of the system to the cavity vector potential, see Eq. (13).

To find the cavity spectral function we first calculate the current-current correlation function using Eqs. (16) and (17). In Fig. 1 (b) we plot the real part of correlation function $\chi'(\omega)$ as a function of frequency ω . Vertical dotted lines indicate the bulk-Majorana transition

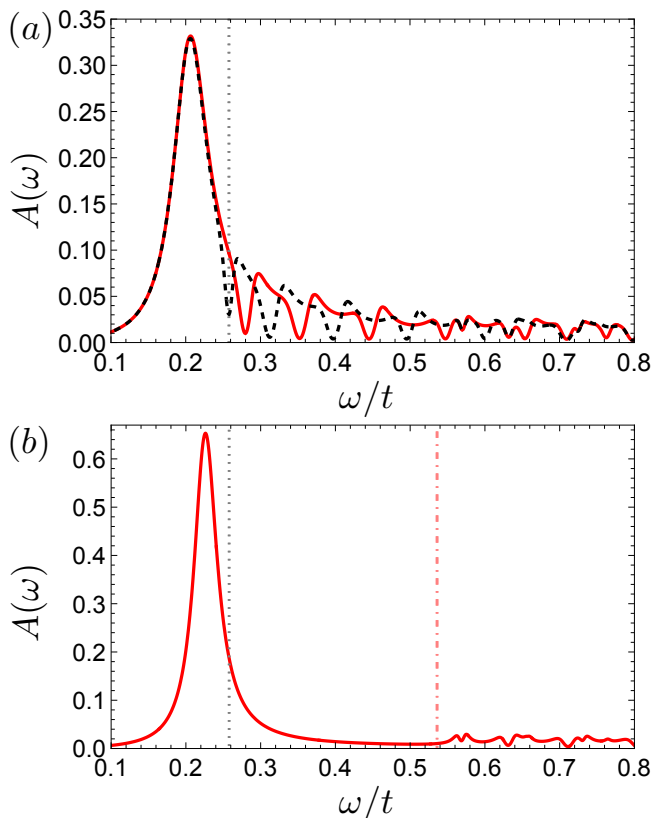


FIG. 2. Cavity spectral function $A(\omega)$ as function of frequency ω/t for $g = 0.1$. (a) In the topological phase ($\mu/t = -1.75$) red solid (black dashed) line corresponds to even (odd) Majorana parity. Vertical gray dotted line indicates the cavity frequency ω_c fixed to be in resonance with the first bulk-Majorana transition. (b) In the trivial phase ($\mu/t = -2.25$) there is a large peak emerging at ω_c and smaller peaks appearing at $\omega > 2\Delta_g$. Vertical gray dotted line corresponds to ω_c and pink dot-dashed line indicates the first bulk-bulk transition. Other parameters are the same as in Fig. 1.

frequencies $\omega_{e(o)}$. For the Kitaev chain in the topological phase $\epsilon_M \approx 0$ and therefore $\omega_e \approx \omega_o$. We find that $\chi'(\omega)$ has different oscillation amplitudes for even and odd Majorana parities stemming from the difference in the matrix elements $j_{l,e}^p$. Next, we numerically evaluate the imaginary part of the correlation function $\chi''(\omega)$ (see Fig. 1 (c)). The function $\chi''(\omega)$ has multiple peaks at resonant frequencies $\omega_{e(o)}$ that differ for two parities, similarly to the features present in $\chi'(\omega)$. Therefore, the current-current correlation function $\chi(\omega)$ is a good marker to distinguish between two Majorana parities in the topological phase.

Given the above results for the current-current correlator we can now focus on the cavity photon spectral function (11). We plot $A(\omega)$ as a function of frequency in Fig. 2 (a) at a fixed light-matter coupling g for different parities in topological phase. The current-current correlation function is calculated for a finite-length Kitaev chain and has many resonances (see Fig. 1 (b)), therefore, Eq. (14) has multiple solutions for polariton energies corresponding to peaks in $A(\omega)$. Moreover, the polariton spectrum in topological phase depends on the Majorana parity through $\chi'(\omega)$. The cavity spectral function has different patterns for two parities and can distinguish between the parities. We further compute the cavity spectral function in the trivial phase [see Fig. 2 (b)] for the same light-matter coupling strength g and the effective gap Δ_g . We find that $A(\omega)$ has a sharp peak around the cavity frequency ω_c as in the topologically nontrivial phase. However, we note that contrary to topological case small peaks emerge at frequencies larger than $2\Delta_g$ corresponding to bulk-bulk transition across the gap in the system.

In Fig. (3) (a) we plot the cavity spectral function for the Kitaev chain in the topological phase as a function of frequency and light-matter coupling. We consider a cavity frequency in resonance with the first bulk-Majorana transition for the even parity ($\omega_c = \omega_e$). We see that for low frequency there is a broad peak which shifts towards lower frequencies upon increasing g . At higher frequencies on the other hand we recognize sharp features associated to transitions between Majorana and bulk states. Next, we calculate $A(\omega)$ for the Kitaev chain in the trivial phase [see Fig. (3) (b)]. As discussed for the topological phase there is a broad peak that originates at $\omega = \omega_c$ for $g = 0$ and further broaden as the light-matter coupling strength is increased. However, in the trivial phase the current-current correlation function $\chi(\omega)$ that enters Eq. (11) has resonances only at frequencies $\omega_b > 2\Delta_g$. Therefore, other polariton modes appear only at $\omega > 2\Delta_g$. Comparing the cavity spectral function calculated in the topological phases we note the distinct features between the two, namely that the sharp features of the transitions between Majorana (bulk) - bulk states appear at different energy scales of Δ_g ($2\Delta_g$). Therefore, the polariton spectrum could be potentially used as a way to probe zero-energy states in topological superconductors.

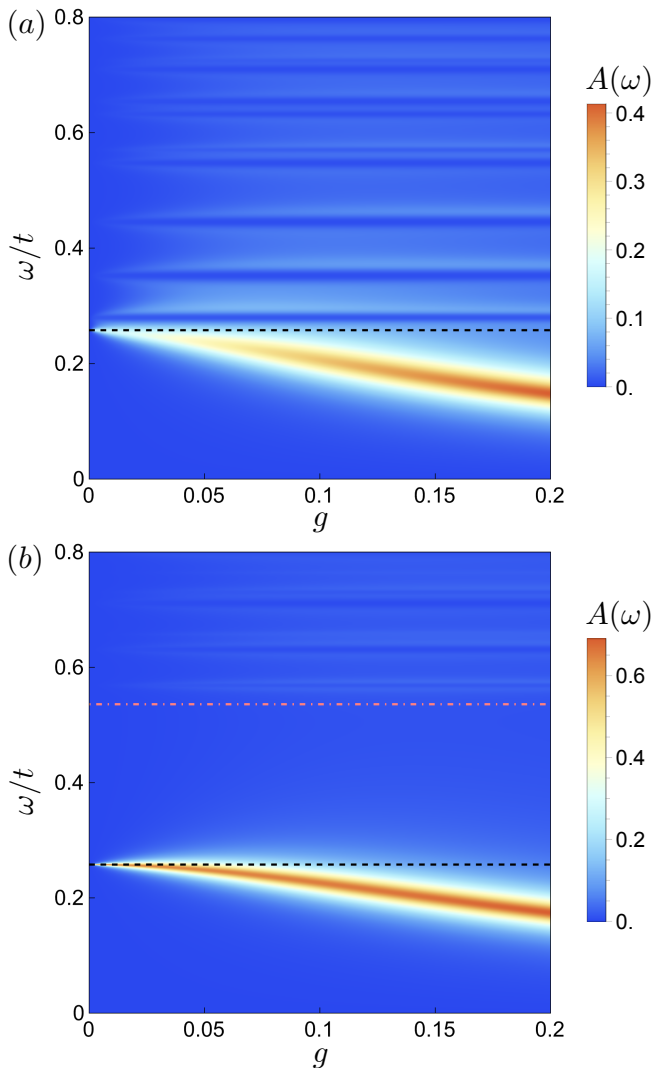


FIG. 3. Spectral function $A(\omega)$ as a function of g and ω/t . Horizontal black dashed line corresponds to frequency ω_c chosen to be equal to first bulk-Majorana transition frequency and horizontal pink dot-dashed line corresponds to ω_b in the trivial phase. (a) In the topological phase with $\mu/t = -1.75$ the lowest polariton branch originating at $\omega = \omega_c$ for $g = 0$ goes down as g is increased. White horizontal lines corresponding to bulk-Majorana transitions coupled with photons that appear at frequencies $\omega > \Delta_g$. (b) In the trivial phase with $\mu/t = -2.25$, the lowest polariton branch appears at $\omega = \omega_c$. In contrast to the topological phase, white horizontal lines correspond to bulk-bulk transitions and appear at $\omega > 2\Delta_g$. In two phases white horizontal lines corresponding to bulk-Majorana (a) and bulk-bulk (b) transitions emerge at different frequencies signalling the presence of zero-energy states in the topological phase. Other parameters are the same as in Fig. 1.

B. Polaritons in nanowire coupled to photons

We now move to the superconductor-semiconductor nanowire model, Eq. (9), for which the paramagnetic and

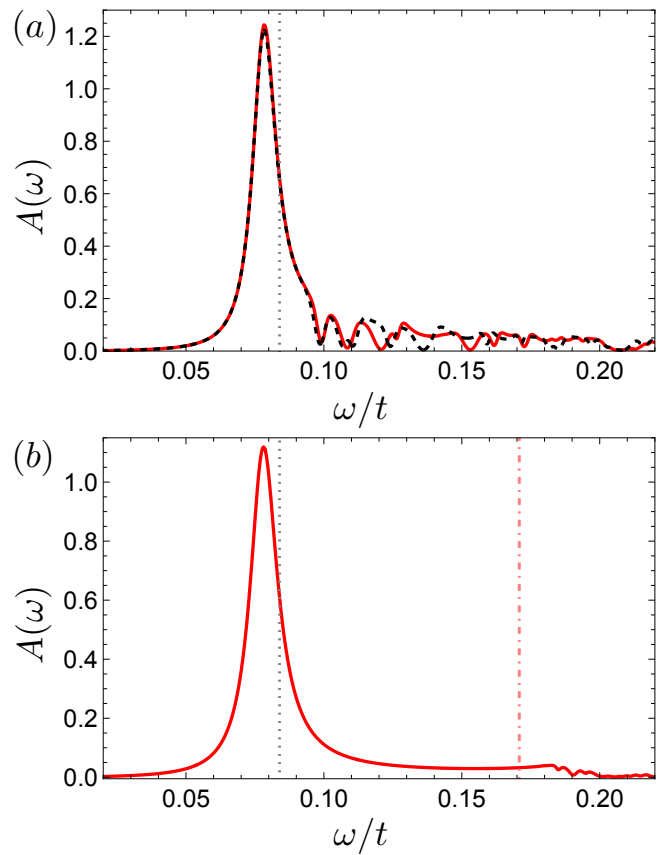


FIG. 4. Cavity spectral function $A(\omega)$ of the nanowire as function of frequency ω/t for light-matter coupling strength $g = 0.05$. (a) Red solid (black dashed) lines correspond to $n_M = 0$ ($n_M = 1$) in the topological phase with $V_Z/\Delta = 1.8$. Gray vertical dotted line indicates the cavity frequency ω_c resonant with the first bulk-Majorana transition at $\omega_e \approx \omega_o$ ($\epsilon_M/t = 10^{-6}$). (b) $A(\omega)$ for the nanowire in the trivial phase with $V_Z/\Delta = 0.2$. Vertical gray dotted line indicates ω_c and pink dot-dashed line signals the position of the first bulk-bulk transition frequency ω_b . Other parameters are fixed as $N = 100$, $\Delta/t = 0.1$, $\mu = 0$, $V_Z/\Delta = 1.8$, $\alpha/t = 0.4$, and $\eta/t = 10^{-3}$.

diamagnetic current operators read respectively

$$J_p = i \frac{g}{\sqrt{N}} \sum_j \left[t \left(c_{j+1\uparrow}^\dagger c_{j\uparrow} + c_{j+1\downarrow}^\dagger c_{j\downarrow} \right) + \alpha \left(c_{j+1\uparrow}^\dagger c_{j\downarrow} - c_{j+1\downarrow}^\dagger c_{j\uparrow} \right) - 2\Delta \chi_j c_{j\uparrow}^\dagger c_{j\downarrow}^\dagger - \text{h.c.} \right] \quad (22)$$

and

$$J_d = \frac{g^2}{N} \sum_j \left[-t \left(c_{j+1\uparrow}^\dagger c_{j\uparrow} + c_{j+1\downarrow}^\dagger c_{j\downarrow} \right) + \alpha \left(c_{j+1\uparrow}^\dagger c_{j\downarrow} - c_{j+1\downarrow}^\dagger c_{j\uparrow} \right) + 4\Delta \chi_j^2 c_{j\uparrow}^\dagger c_{j\downarrow}^\dagger + \text{h.c.} \right]. \quad (23)$$

To find the cavity spectral function of the nanowire model, we proceed in the same way as for the Kitaev chain. The real and imaginary part of $\chi(\omega)$ has similar

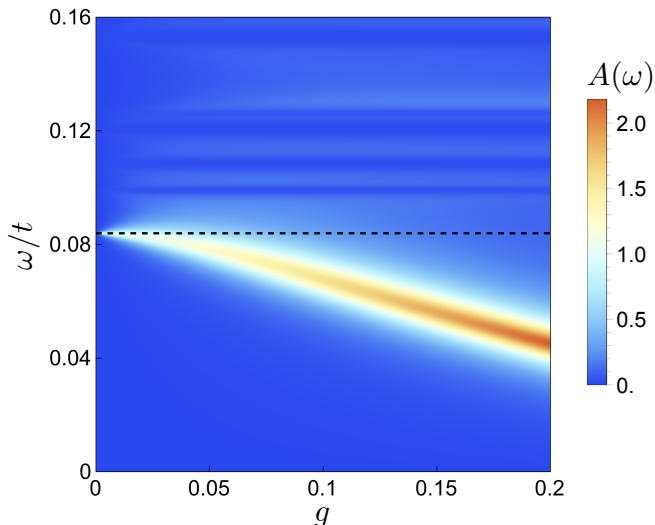


FIG. 5. Cavity spectral function $A(\omega)$ of the nanowire as a function of the light-matter coupling g and frequency ω/t . Black dashed line indicates the value of cavity frequency $\omega_c = \omega_e$ (resonant with the first bulk-Majorana transition for even parity). White horizontal lines correspond to bulk-Majorana transitions and emerge at frequencies $\omega > \Delta_g$. Other parameters are same as in Fig. 4.

structure to Fig. 1, but the position and amplitude of the peaks are less homogeneous due to more involved energy spectrum of the nanowire.

In Fig. 4 we plot the cavity spectral function for the nanowire model as a function of frequency ω for a fixed value of the light-matter coupling g . In the topological phase we consider different parities depicted in solid red and black dashed line. The cavity spectral function has a large peak around the cavity frequency ω_c resonant with the lowest bulk-Majorana transition frequency $\omega_e \approx \omega_o$ and multiple smaller peaks corresponding to higher in energy bulk-Majorana transitions appearing at $\omega > \Delta_g$ [see Fig. 4 (a)]. Considering the superconductor-semiconductor nanowire in the trivial phase coupled to photonic cavity, we find that the cavity spectral function has a sharp peak originating at the frequency ω_c and multiple smaller peaks at frequencies $\omega > 2\Delta_g$ that

stem from the bulk-bulk transitions in the nanowire [see Fig. 4 (b)]. Similar features were found for the Kitaev chain [see Fig. 2 (b)] and allow one to probe the presence of zero-energy modes in the topological superconductor.

Finally, we present $A(\omega)$ for the nanowire in the topological phase as a function of frequency and light-matter coupling strength in Fig. 5. By choosing the cavity frequency to be equal to the first bulk-Majorana transition frequency, we find the appearance of a broad low-frequency polariton mode that goes down in ω with increasing g . Higher-frequency polariton modes appear due to coupling between higher bulk-Majorana transitions and photons showing a dense pattern of modes. Similar behaviour was found for the Kitaev chain (see Fig. 3).

IV. CONCLUSIONS

In this work, we studied the topological superconductor coupled to cavity photons. We calculated the cavity spectral function of the electron-photon system that revealed the polariton spectrum of the hybrid system. The peaks in cavity spectral function appear at different energy scales for the electronic chain in the trivial and topological phase. Moreover, in the topological phase associated with the presence of the Majorana bound states the polariton spectrum has different pattern for two Majorana parities. Therefore, cavity spectral function could be used to probe topological properties of the electronic chain.

ACKNOWLEDGMENTS

O.D. acknowledges helpful discussions with Jelena Klinovaja, Daniel Loss, Pascal Simon and Mircea Trif. This project has received funding from the European Union's Horizon 2020 research and innovation programme under the Marie Skłodowska-Curie grant agreement No 892800. This project has received funding from the European Research Council (ERC) under the European Union's Horizon 2020 research and innovation programme (Grant agreement No. 101002955 — CONQUER).

-
- [1] F. J. Garcia-Vidal, C. Ciuti, and T. W. Ebbesen, Manipulating matter by strong coupling to vacuum fields, *Science* **373**, eabd0336 (2021).
 - [2] F. Schlawin, D. M. Kennes, and M. A. Sentef, Cavity quantum materials, *Applied Physics Reviews* **9** (2022).
 - [3] J. J. Hopfield, Theory of the contribution of excitons to the complex dielectric constant of crystals, *Phys. Rev.* **112**, 1555 (1958).
 - [4] D. N. Basov, A. Asenjo-Garcia, P. J. Schuck, X. Zhu, and A. Rubio, Polariton panorama, *Nanophotonics* **10**, 549 (2021).
 - [5] C. Ciuti, Cavity-mediated electron hopping in disordered quantum Hall systems, *Phys. Rev. B* **104**, 155307 (2021).
 - [6] F. Appugliese, J. Enkner, G. L. Paravicini-Bagliani, M. Beck, C. Reichl, W. Wegscheider, G. Scalari, C. Ciuti, and J. Faist, Breakdown of topological protection by cavity vacuum fields in the integer quantum Hall effect, *Science* **375**, 1030 (2022).
 - [7] O. Dmytruk and M. Schirò, Controlling topological phases of matter with quantum light, *Communications Physics* **5**, 271 (2022).

- [8] B. Pérez-González, G. Platero, and Álvaro Gómez-León, Light-matter correlations in quantum Floquet engineering (2023), arXiv:2302.12290 [cond-mat.mes-hall].
- [9] D. Shaffer, M. Claassen, A. Srivastava, and L. H. Santos, Entanglement and topology in Su-Schrieffer-Heeger cavity quantum electrodynamics (2023), arXiv:2308.08588 [cond-mat.str-el].
- [10] T. Karzig, C.-E. Bardyn, N. H. Lindner, and G. Refael, Topological polaritons, *Phys. Rev. X* **5**, 031001 (2015).
- [11] A. Y. Kitaev, Unpaired Majorana fermions in quantum wires, *Physics-Uspekhi* **44**, 131 (2001).
- [12] J. Alicea, New directions in the pursuit of Majorana fermions in solid state systems, *Reports on Progress in Physics* **75**, 076501 (2012).
- [13] C. Beenakker, Search for Majorana fermions in superconductors, *Annual Review of Condensed Matter Physics* **4**, 113 (2013).
- [14] E. Prada, P. San-Jose, M. W. A. de Moor, A. Geresdi, E. J. H. Lee, J. Klinovaja, D. Loss, J. Nygård, R. Aguado, and L. P. Kouwenhoven, From Andreev to Majorana bound states in hybrid superconductor–semiconductor nanowires, *Nature Reviews Physics* **2**, 575 (2020).
- [15] S. D. Sarma, M. Freedman, and C. Nayak, Majorana zero modes and topological quantum computation, *npj Quantum Information* **1**, 15001 (2015).
- [16] R. M. Lutchyn, J. D. Sau, and S. Das Sarma, Majorana fermions and a topological phase transition in semiconductor-superconductor heterostructures, *Phys. Rev. Lett.* **105**, 077001 (2010).
- [17] Y. Oreg, G. Refael, and F. von Oppen, Helical liquids and Majorana bound states in quantum wires, *Phys. Rev. Lett.* **105**, 177002 (2010).
- [18] C. Dutreix, M. Guigou, D. Chevallier, and C. Bena, Majorana fermions in honeycomb lattices, *The European Physical Journal B* **87**, 296 (2014).
- [19] P. San-Jose, J. L. Lado, R. Aguado, F. Guinea, and J. Fernández-Rossier, Majorana zero modes in graphene, *Phys. Rev. X* **5**, 041042 (2015).
- [20] S. Nadj-Perge, I. K. Drozdov, B. A. Bernevig, and A. Yazdani, Proposal for realizing Majorana fermions in chains of magnetic atoms on a superconductor, *Phys. Rev. B* **88**, 020407(R) (2013).
- [21] J. Klinovaja, P. Stano, A. Yazdani, and D. Loss, Topological superconductivity and Majorana fermions in RKKY systems, *Phys. Rev. Lett.* **111**, 186805 (2013).
- [22] B. Braunecker and P. Simon, Interplay between classical magnetic moments and superconductivity in quantum one-dimensional conductors: Toward a self-sustained topological Majorana phase, *Phys. Rev. Lett.* **111**, 147202 (2013).
- [23] V. Mourik, K. Zuo, S. M. Frolov, S. R. Plissard, E. P. A. M. Bakkers, and L. P. Kouwenhoven, Signatures of Majorana fermions in hybrid superconductor-semiconductor nanowire devices, *Science* **336**, 1003 (2012).
- [24] M. T. Deng, C. L. Yu, G. Y. Huang, M. Larsson, P. Caroff, and H. Q. Xu, Anomalous zero-bias conductance peak in a Nb–InSb nanowire–Nb hybrid device, *Nano Letters* **12**, 6414 (2012).
- [25] A. Das, Y. Ronen, Y. Most, Y. Oreg, M. Heiblum, and H. Shtrikman, Zero-bias peaks and splitting in an Al–InAs nanowire topological superconductor as a signature of Majorana fermions, *Nature Physics* **8**, 887 (2012).
- [26] H. O. H. Churchill, V. Fatemi, K. Grove-Rasmussen, M. T. Deng, P. Caroff, H. Q. Xu, and C. M. Marcus, Superconductor-nanowire devices from tunneling to the multichannel regime: Zero-bias oscillations and magnetoconductance crossover, *Phys. Rev. B* **87**, 241401(R) (2013).
- [27] M. T. Deng, S. Vaitiekėnas, E. B. Hansen, J. Danon, M. Leijnse, K. Flensberg, J. Nygård, P. Krogstrup, and C. M. Marcus, Majorana bound state in a coupled quantum-dot hybrid-nanowire system, *Science* **354**, 1557 (2016).
- [28] M. W. A. de Moor, J. D. S. Bommer, D. Xu, G. W. Winkler, A. E. Antipov, A. Bargerbos, G. Wang, N. van Loo, R. L. M. O. het Veld, S. Gazibegovic, D. Car, J. A. Logan, M. Pendharkar, J. S. Lee, E. P. A. M. Bakkers, C. J. Palmstrøm, R. M. Lutchyn, L. P. Kouwenhoven, and H. Zhang, Electric field tunable superconductor-semiconductor coupling in Majorana nanowires, *New Journal of Physics* **20**, 103049 (2018).
- [29] M. Aghaee, A. Akkala, Z. Alam, R. Ali, A. Alcaraz Ramirez, M. Andrzejczuk, A. E. Antipov, P. Aseev, M. Astafev, B. Bauer, and *et al.* (Microsoft Quantum), InAs-Al hybrid devices passing the topological gap protocol, *Phys. Rev. B* **107**, 245423 (2023).
- [30] G. Kells, D. Meidan, and P. W. Brouwer, Near-zero-energy end states in topologically trivial spin-orbit coupled superconducting nanowires with a smooth confinement, *Phys. Rev. B* **86**, 100503(R) (2012).
- [31] C.-X. Liu, J. D. Sau, T. D. Stanescu, and S. Das Sarma, Andreev bound states versus Majorana bound states in quantum dot-nanowire-superconductor hybrid structures: Trivial versus topological zero-bias conductance peaks, *Phys. Rev. B* **96**, 075161 (2017).
- [32] A. Ptok, A. Kobińska, and T. Domański, Controlling the bound states in a quantum-dot hybrid nanowire, *Phys. Rev. B* **96**, 195430 (2017).
- [33] F. Setiawan, C.-X. Liu, J. D. Sau, and S. Das Sarma, Electron temperature and tunnel coupling dependence of zero-bias and almost-zero-bias conductance peaks in Majorana nanowires, *Phys. Rev. B* **96**, 184520 (2017).
- [34] C. Moore, T. D. Stanescu, and S. Tewari, Two-terminal charge tunneling: Disentangling Majorana zero modes from partially separated Andreev bound states in semiconductor-superconductor heterostructures, *Phys. Rev. B* **97**, 165302 (2018).
- [35] C. Reeg, O. Dmytruk, D. Chevallier, D. Loss, and J. Klinovaja, Zero-energy Andreev bound states from quantum dots in proximitized Rashba nanowires, *Phys. Rev. B* **98**, 245407 (2018).
- [36] A. Vuik, B. Nijholt, A. R. Akhmerov, and M. Wimmer, Reproducing topological properties with quasi-Majorana states, *SciPost Phys.* **7**, 061 (2019).
- [37] R. Hess, H. F. Legg, D. Loss, and J. Klinovaja, Local and nonlocal quantum transport due to Andreev bound states in finite Rashba nanowires with superconducting and normal sections, *Phys. Rev. B* **104**, 075405 (2021).
- [38] R. Hess, H. F. Legg, D. Loss, and J. Klinovaja, Trivial Andreev band mimicking topological bulk gap reopening in the nonlocal conductance of long Rashba nanowires, *Phys. Rev. Lett.* **130**, 207001 (2023).
- [39] A. Cottet, T. Kontos, and B. Douçot, Squeezing light with Majorana fermions, *Phys. Rev. B* **88**, 195415 (2013).
- [40] O. Dmytruk, M. Trif, and P. Simon, Cavity quantum electrodynamics with mesoscopic topological supercon-

- ductors, *Phys. Rev. B* **92**, 245432 (2015).
- [41] O. Dmytruk, M. Trif, and P. Simon, Josephson effect in topological superconducting rings coupled to a microwave cavity, *Phys. Rev. B* **94**, 115423 (2016).
- [42] M. C. Dartiailh, T. Kontos, B. Douçot, and A. Cottet, Direct cavity detection of Majorana pairs, *Phys. Rev. Lett.* **118**, 126803 (2017).
- [43] A. Cottet, M. C. Dartiailh, M. M. Desjardins, T. Cubaynes, L. C. Contamin, M. Delbecq, J. J. Viennot, L. E. Bruhat, B. Douçot, and T. Kontos, Cavity QED with hybrid nanocircuits: from atomic-like physics to condensed matter phenomena, *Journal of Physics: Condensed Matter* **29**, 433002 (2017).
- [44] M. Trif, O. Dmytruk, H. Bouchiat, R. Aguado, and P. Simon, Dynamic current susceptibility as a probe of Majorana bound states in nanowire-based Josephson junctions, *Phys. Rev. B* **97**, 041415(R) (2018).
- [45] M. Trif and P. Simon, Braiding of Majorana fermions in a cavity, *Phys. Rev. Lett.* **122**, 236803 (2019).
- [46] O. Dmytruk and M. Trif, Microwave detection of gliding Majorana zero modes in nanowires, *Phys. Rev. B* **107**, 115418 (2023).
- [47] Z. Ren, J. Copenhaver, L. Rokhinson, and J. I. Väyrynen, Microwave spectroscopy of Majorana vortex modes (2023), arXiv:2309.04050 [cond-mat.supr-con].
- [48] M. Trif and Y. Tserkovnyak, Resonantly tunable Majorana polariton in a microwave cavity, *Phys. Rev. Lett.* **109**, 257002 (2012).
- [49] Z. Bacciconi, G. M. Andolina, and C. Mora, Topological protection of Majorana polaritons in a cavity (2023), arXiv:2309.07278 [cond-mat.mes-hall].
- [50] G. Mazza and A. Georges, Superradiant quantum materials, *Phys. Rev. Lett.* **122**, 017401 (2019).
- [51] I. Amelio, L. Korosec, I. Carusotto, and G. Mazza, Optical dressing of the electronic response of two-dimensional semiconductors in quantum and classical descriptions of cavity electrodynamics, *Phys. Rev. B* **104**, 235120 (2021).
- [52] O. Dmytruk and M. Schiró, Gauge fixing for strongly correlated electrons coupled to quantum light, *Phys. Rev. B* **103**, 075131 (2021).
- [53] E. Vlasiuk, V. K. Kozin, J. Klinovaja, D. Loss, I. V. Iorsh, and I. V. Tokatly, Cavity-induced charge transfer in periodic systems: Length-gauge formalism, *Phys. Rev. B* **108**, 085410 (2023).
- [54] B. Pérez-González, Á. Gómez-León, and G. Platero, Topology detection in cavity QED, *Physical Chemistry Chemical Physics* **24**, 15860 (2022).
- [55] F. Pientka, A. Romito, M. Duckheim, Y. Oreg, and F. von Oppen, Signatures of topological phase transitions in mesoscopic superconducting rings, *New Journal of Physics* **15**, 025001 (2013).
- [56] A. Cottet, T. Kontos, and B. Douçot, Electron-photon coupling in mesoscopic quantum electrodynamics, *Phys. Rev. B* **91**, 205417 (2015).
- [57] O. Dmytruk and J. Klinovaja, Suppression of the overlap between Majorana fermions by orbital magnetic effects in semiconducting-superconducting nanowires, *Phys. Rev. B* **97**, 155409 (2018).
- [58] P. Nataf, T. Champel, G. Blatter, and D. M. Basko, Rashba cavity QED: A route towards the superradiant quantum phase transition, *Phys. Rev. Lett.* **123**, 207402 (2019).
- [59] G. M. Andolina, F. M. D. Pellegrino, V. Giovannetti, A. H. MacDonald, and M. Polini, Cavity quantum electrodynamics of strongly correlated electron systems: A no-go theorem for photon condensation, *Phys. Rev. B* **100**, 121109(R) (2019).
- [60] D. Guerçi, P. Simon, and C. Mora, Superradiant phase transition in electronic systems and emergent topological phases, *Phys. Rev. Lett.* **125**, 257604 (2020).
- [61] G. M. Andolina, F. M. D. Pellegrino, V. Giovannetti, A. H. MacDonald, and M. Polini, Theory of photon condensation in a spatially varying electromagnetic field, *Phys. Rev. B* **102**, 125137 (2020).